

Development of second harmonic gyrotrons, Gyrotron FU CW GII and Gyrotron FU CW GIII, equipped with internal mode converters

Yoshinori Tatematsu · Yuusuke Yamaguchi ·
Toshitaka Idehara · Tatsuru Kawase · Ryoichi Ichioka ·
Isamu Ogawa · Teruo Saito · Toshimichi Fujiwara

Received: 5 November 2013 / Accepted: 6 January 2014 /
Published online: 15 January 2014
© Springer Science+Business Media New York 2014

Abstract Second harmonic gyrotrons, Gyrotron FU CW GII and Gyrotron FU CW GIII, were developed at the Research Center for Development of Far-Infrared Region, University of Fukui, Japan to achieve two goals. Each gyrotron was equipped with an internal quasi-optical mode converter. Using Gyrotron FU CW GII allowed the design of the cavity and mode converter to be validated, which was the first goal. After that, Gyrotron FU CW GIII, which is an improved version of Gyrotron FU CW GII, allowed us to achieve a high power output of up to 420 W, which was the second goal, with a cathode voltage setting of -21 kV and a beam current of 0.57 A. This was achieved using a newly developed electron gun and with the careful sitting of the gyrotron on the magnet.

Keywords Gyrotron · Gaussian beam · Mode converter · High power radiation source · Second harmonic resonance

1 Introduction

Gyrotrons equipped with quasi-optical mode converters (Gyrotron FU CW G series) have been developed at the Research Center for Development of Far-Infrared Region, University of Fukui, Japan [1]. One of these gyrotrons is called Gyrotron FU CW GI, and it operates at a fundamental harmonic frequency of around 203 GHz. It has been used as a radiation source for measuring positronium hyperfine splitting [2, 3], as a successor of Gyrotron FU CW V [4], which was successfully used for the first direct measurement of the level transition of positronium from an ortho state to a para state through a stimulated emission process [5]. Following the development of Gyrotron FU CW GI, a second gyrotron, Gyrotron FU CW GII, which has a mode converter, was developed. This gyrotron oscillates at the second harmonic

Y. Tatematsu (✉) · Y. Yamaguchi · T. Idehara · T. Kawase · R. Ichioka · I. Ogawa · T. Saito
Research Center for Development of Far-Infrared Region, University of Fukui, Fukui 910-8507, Japan
e-mail: tatemala@fir.u-fukui.ac.jp

T. Fujiwara
Institute for Protein Research, Osaka University, Osaka 565-0871, Japan

cyclotron resonance and, consequently, the frequency is almost twice that of Gyrotron FU CW GI.

A high-power electromagnetic (EM) wave with a sub-THz frequency range can be used for proton dynamical nuclear polarization (DNP) nuclear magnetic resonance (NMR) spectroscopy, [6], for which a source power of more than 10 W is required. We have developed gyrotrons with frequencies of around 400 GHz, such as Gyrotron FU CW II, Gyrotron FU CW VI, and Gyrotron FU CW VII, for use as radiation sources for this application [7–9]. However, those gyrotrons were of the linear type, in which the vacuum window is located at the top of the gyrotron and the EM wave field radiated through it has a complex structure and zero strength along its axis. Such a complex field structure is not suitable for applications that require efficient transmission over a long distance. Therefore, it is desirable to develop a gyrotron that directly produces a Gaussian beam with linear polarization, so Gyrotron FU CW GII was developed.

The first goal in developing Gyrotron FU CW GII was to validate the method for designing a second harmonic gyrotron with a mode converter. There are several constraints on the design process. In particular, a room-temperature bore with a small diameter of 100 mm for the superconducting magnet (SCM) is a severe constraint. A very small space remained for the internal mode converter once the paths for the water cooling system and for evacuating the gun region had been chosen. The cavity dimension, the oscillation mode, and the structure of the mode converter were optimized for these conditions.

The electron optics needs to be optimized to achieve high efficiency oscillations. However, we initially used an existing electron gun design to validate the design procedures for the cavity and the mode converter. Although this resulted in a rather low maximum power, 74 W, in experiments using Gyrotron FU CW GII, the cavity and mode converter designs were found to be consistent, from measurements of the beam pattern radiated from the window.

The power achieved, 74 W, was high enough for use in DNP-NMR spectroscopy experiments, so Gyrotron FU CW GII was sent to Osaka University, Japan for use in their DNP-NMR spectroscopy experiments.

The second goal, improving the gyrotron power, was assigned to a new gyrotron. The power achieved in experiments using Gyrotron FU CW GII was much lower than expected from calculations, a power more than a few hundred watts being expected using the chosen operating parameters. We thought that the power limitation was caused by the electron gun, because it was not optimized for this gyrotron.

Gyrotron FU CW GIII was developed as an improved version of Gyrotron FU CW GII. One of the improvements was that a new electron gun was specifically designed for Gyrotron FU CW GIII, to achieve a higher power than was achieved using Gyrotron FU CW GII. Moreover, the gyrotron was carefully aligned on the SCM for the same reason.

In this paper, we will describe (in section 2) the design of Gyrotron FU CW GII, experimental results using it, and how they matched our first goal. We will then describe (in section 3) the design of Gyrotron FU CW GIII, experimental results using it, and how they matched our second goal.

2 Gyrotron FU CW GII

The cavity dimension and the oscillation mode should be carefully determined to achieve both oscillation at the required frequency and compatibility with the mode converter that is installed in the narrow space available. We designed Gyrotron FU CW GII using a procedure similar to that used for Gyrotron FU CW GI [1]. The co-rotating $TE_{8,3}$ mode was selected and the cavity

dimensions of the straight section were a radius of 2.15 mm and a length of 17 mm. These dimensions were determined for the gyrotron tube, which contains the cavity and the mode converter, and which was placed within the 100 mm diameter room-temperature bore of an 8 T-SCM. The range of the Brillouin angle of the oscillation mode was carefully considered so that it would be compatible with the mode converter designed for the narrow space. The oscillation power was calculated using a mode competition code in which time-dependent equations for the oscillation amplitudes were solved and the axial field profiles were self-consistently determined, with interactions between the electron beam and the RF fields. Figure 1 shows the calculated oscillation power P_{cav} at the cavity exit as a function of the cavity magnetic field strength B for the co-TE_{8,3} mode and its competing modes. The second harmonic ctr-TE_{3,5} mode, the fundamental co-TE_{4,2} mode and the ctr-TE_{1,3} mode were taken into account as competing modes. In the calculations, the cathode voltage V_k was -15 kV, the beam current I_b was 0.5 A, the pitch factor α was 1.2, with no velocity spread, and the electron guiding center radius R_b was 0.91 mm. The thickness of the electron beam was not considered. Although the TE_{8,3} mode had several competing modes, it could oscillate as a single mode as long as R_b was set at an appropriate value. A maximum P_{cav} value of about 0.6 kW was expected.

The quasi-optical mode converter consisted of a Vlasov launcher, and included a conventional helical cut waveguide, a quasi-parabolic mirror, two plane mirrors, and one elliptical mirror. The elliptical mirror could be rotated horizontally and vertically, and it could be translated along the direction of the radiation power.

The electron gun was not specifically designed for this gyrotron, but for another gyrotron similar to Gyrotron FU CW GI. Gun coils were installed to modify the magnetic field distribution near the electron gun. Properly tuning the gun coil current I_g allowed the electron radius R_b at the cavity entrance to be set to the optimal value.

A photograph of Gyrotron FU CW GII, which is a sealed-off type gyrotron, is shown in Fig. 2. The gyrotron was installed on a liquid He-free 8 T-SCM. At first, we searched for the oscillation signal for the design mode TE_{8,3}, which was expected to oscillate around 7.2 T, from the TE_{8,3} mode power calculation as shown in Fig. 1. The radiation signal intensity, measured using a pyro-electric detector placed in front of the sapphire window, is shown in Fig. 3. The setting cathode voltage V_{k0} and gun coil current I_g were -17 kV and 214.6 A, respectively. The actual cathode voltage was about -16 kV because of the voltage drop caused by the series resistance between the power supply and the cathode. The oscillation signal was

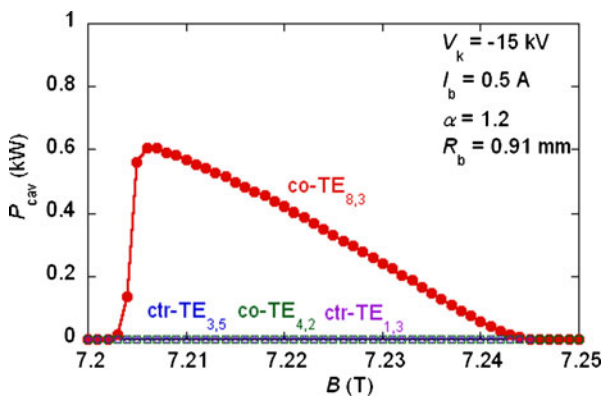


Fig. 1 Power calculation with a mode competing code



Fig. 2 Photograph of Gyrotron FU CW GII mounted on an 8 T superconducting magnet

actually detected in the expected magnetic field strength range. The frequency was measured using a heterodyne receiver system, and it was found to be 393.4 GHz. This frequency was found to correspond to a cavity radius of 2.157 mm, using the cold cavity calculation. Therefore, we considered that the actual radius was a little larger than the 2.15 mm specified in the design.

A radiation pattern for the EM wave emitted through the window was measured as the temperature increase on a vinyl chloride plate placed in front of the window, using an IR camera, and the pattern found is shown in Fig. 4. The length of each side of Fig. 4 is 100 mm and the plate was located 175 mm from the window. It can be seen that the pattern was circular. We performed polarization measurements on this wave by placing a polarizer, consisting of parallel metal wires, in front of the window. The wave signal intensity through the polarizer was detected using a pyro-electric detector. The direction of the metal wires was rotated and variations in the intensity were observed. The signal intensity is plotted against the polarizer rotation angle, θ , in Fig. 5, in which θ is the angle between the wire direction and a vertical line. The dependence of the observed signal on θ matches $\cos^2\theta$, which means that the polarization was almost linear. The electric field was horizontal, as expected.

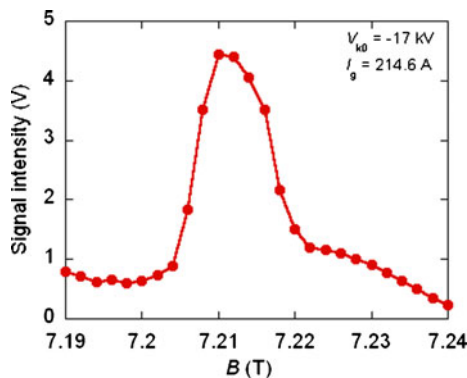


Fig. 3 Measured signal intensity plotted against the magnetic field strength at the cavity

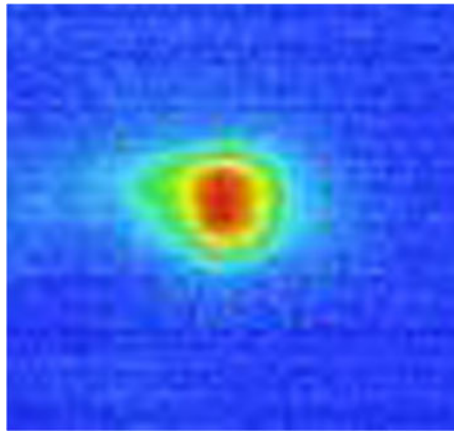


Fig. 4 Radiation pattern from Gyrotron FU CW GII

The window power was then measured using a water load system. We changed the operating conditions, such as the anode voltage and the gun coil current, to increase the power. Figure 6 shows the maximum observed power for each cathode voltage (V_{k0}) setting. A maximum power of 74 W was obtained when V_{k0} was -19 or -20 kV.

The experimental results showed that this gyrotron had the properties necessary for it to be used as a radiation source in DNP-NMR spectroscopy experiments.

3 Gyrotron FU CW GIII

The maximum power of Gyrotron FU CW GII was 74 W, but we expected an output power of at least a few hundred watts, even when transmission losses through the mode converter and window were subtracted from the calculated oscillation power of 0.6 kW. It is likely that one of the causes for the observed power being much lower than expected was the electron gun, because it was not specifically designed for the gyrotron.

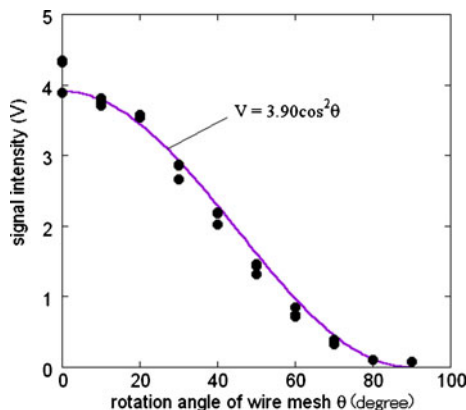


Fig. 5 Polarization measurements of the radiated EM wave

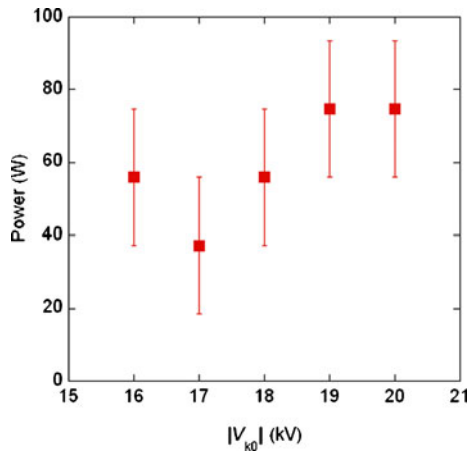


Fig. 6 Measured maximum window power for each V_{k0}

After our initial experiments, Gyrotron FU CW GII was sent to Osaka University for use in DNP-NMR spectroscopy experiments, so we then designed a new gyrotron, Gyrotron FU CW GIII. The design parameters for this gyrotron were almost the same as those for Gyrotron FU CW GII, but the cavity radius was 2.1495 mm, which is slightly smaller than the cavity radius in Gyrotron FU CW GII. An improvement on the Gyrotron FU CW GII was that a new magnetron injection gun was designed specifically for Gyrotron FU CW GIII, and window and mirror cooling systems were added so that a high power and completely continuous wave operation could be achieved.

The goal of developing Gyrotron FU CW GIII was to verify the design calculations on the basis of the output power. Therefore, optimizing the electron beam quality was the key factor that would indicate our success achieving this goal. A new electron gun was designed using the EGUN code. The electrode configurations were optimized by laminating the electron trajectories and by decreasing the spread, $\Delta\alpha$, of the pitch factor (α) of the electron beam at the cavity entrance [10, 11]. $\Delta\alpha$ was decreased from more than 30 % in Gyrotron FU CW GII to 7 % in Gyrotron FU CW GIII [12].

A photograph of Gyrotron FU CW GIII before it was installed in the SCM is shown in Fig. 7. The gyrotron was mounted on the same SCM as was used for the Gyrotron FU CW GII experiments. The beam pattern radiating from the window was measured in the initial Gyrotron FU CW GIII experiments using an IR camera, and the pattern is shown in Fig. 8. The target plate was placed 140 mm from the window and the length of one side of Fig. 8 is 50 mm. We then performed a parameter search for the oscillation conditions, and a maximum power of 190 W was found at $V_{k0} = -20$ kV and $I_b = -0.5$ A. This power was higher than that obtained using Gyrotron FU CW GII, but it was still lower than expected. The alignment between the gyrotron and the coil axes affects the oscillation power [13, 14], so we installed the gyrotron on the SCM carefully. However, it is likely that we had not been careful enough and that the alignment was insufficiently accurate.

We calculated the oscillation power including the misalignment to evaluate the misalignment effect [15]. This calculation evaluates the effect of misalignment in the same manner as that used previously [14]. Here, we assumed that a circular electron beam was injected into the cavity with some displacement from the cavity center. The deviation d was determined as the distance between the injection annular electron beam and cavity center axes. The maximum



Fig. 7 Photograph of Gyrotron FU CW GIII

calculated power is plotted as a function of d in Fig. 9, in which the given parameters used in the calculations, such as V_k , are the same as those used in Fig. 1. The oscillation power decreased remarkably under these conditions when the deviation d exceeded 0.2 mm, and,

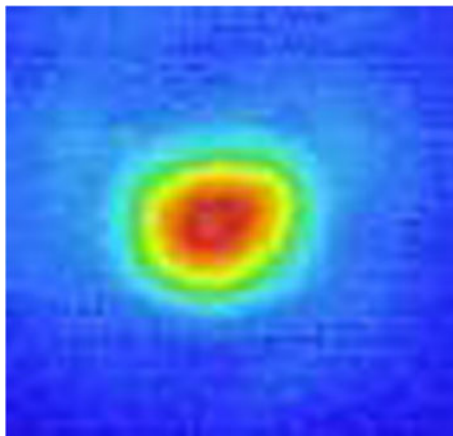


Fig. 8 Measured radiation pattern from Gyrotron FU CW GIII

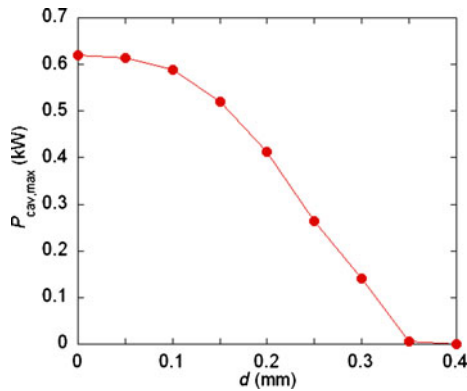


Fig. 9 Calculated maximum oscillation power for the $TE_{8,3}$ mode, including the misalignment effect

finally, the oscillation of the $TE_{8,3}$ mode was lost when d was 0.35 mm, and, instead, the $TE_{3,5}$ mode oscillated.

We carefully set up the gyrotron on the SCM again to attempt to achieve its full potential power. We manufactured a tool to align the gyrotron precisely on the SCM, and we could set the gyrotron position to within 0.1 mm of the desired position on the horizontal top surface of the SCM using this tool. We fine-tuned the gyrotron position by monitoring the power emitted through the window. The observed power was plotted, when the gyrotron was moved in one direction (x -axis) along the surface, and the relationship between the position and the power is shown in Fig. 10, in which $x=0$ mm represents the gyrotron position when the measurements were started. The displacement d is not exactly same as the gyrotron movement x . We calculated the guiding center trajectories of the electrons emitted from the electron gun as the gyrotron was moved perpendicularly to the magnetic coil axis. We found the relationship $dd/dx=0.85$. The results shown in Figs. 9 and 10 are consistent when this relationship is applied. Using these measurements we obtained the maximum power at $x=0.4$ mm. We then moved the gyrotron in the perpendicular direction (the y -direction) to find the optimal position, and the oscillation signal intensity and frequency were measured again at this position. The oscillation signal intensity and frequency at the optimal position are plotted in Fig. 11, in which

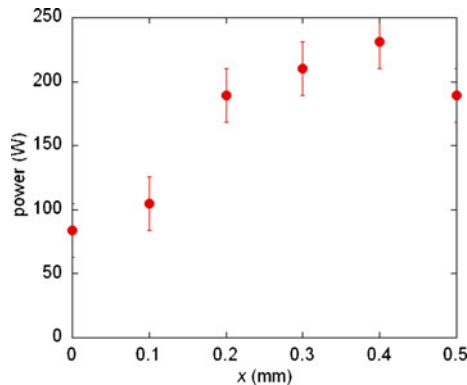


Fig. 10 Observed power through the window as the gyrotron was moved along the SCM surface

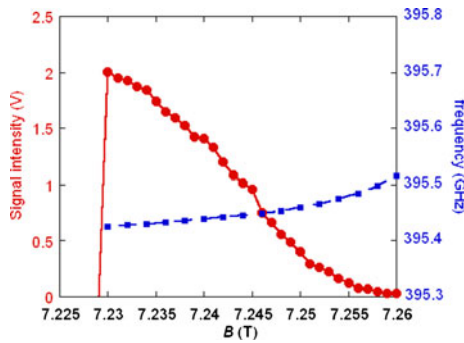


Fig. 11 Measured wave intensity (solid line) and frequency (dashed line) after careful positioning of the gyrotron

the solid and dashed lines indicate the intensity and the frequency, respectively. A continuously changing frequency was found, and the change in frequency (from 395.43 to 395.51 GHz) as B was varied within the tested range is shown in Fig.11. From the frequencies measured, we determined that the $TE_{8,3}$ mode oscillated over the whole range of B values that were tested.

We then optimized other parameters such as the gun coil current and the anode voltage, to obtain a high power. The maximum observed power for each V_{k0} is indicated by closed squares in Fig. 12. The power through the window exceeded the expected few hundred watts in these experiments, and a maximum power of 420 W was found when V_{k0} was -21 kV and I_b was 0.57A. The maximum energy conversion efficiency was found to be 4.3 % when V_{k0} was -16 kV. The observed power from Gyrotron FU CW GII (filled circles) and from the initial Gyrotron FU CW GIII experiment (filled diamonds) are also plotted in Fig. 12. The power obtained from Gyrotron FU CW GIII was more than five times higher than was obtained from Gyrotron FU CW GII and about twice that obtained from the initial Gyrotron FU CW GIII experiment. Therefore, the power output from Gyrotron FU CW GIII can be seen to have been successfully increased. Gyrotron FU CW GIII will be used as a radiation source in a pulsed ESR experiment at the Research Center for Development of Far-Infrared Region at the University of Fukui in the near future.

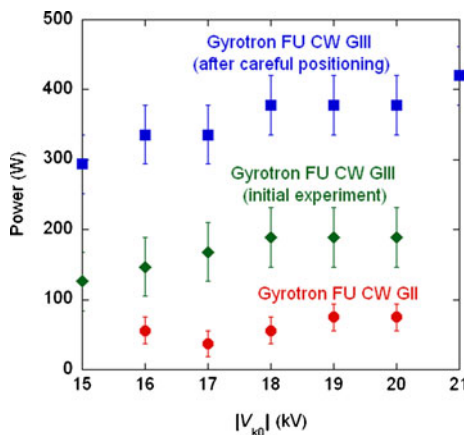


Fig. 12 Measured power through the window from Gyrotron FU CW GII and Gyrotron FU CW GIII

4 Summary

We developed Gyrotron FU CW GII and Gyrotron FU CW GIII, which oscillate at the second harmonic resonance and are equipped with internal mode converters, and achieved two goals, the validation of our design and the verification of the output power that can be achieved. We confirmed that each gyrotron radiates a circular beam from its window. The operations of the gyrotrons were tested, and a 0.074 kW power output and a frequency of 393.4 GHz were found for Gyrotron FU CW GII, which has already been used as a radiation source for 600 MHz DNP-NMR spectroscopy at Osaka University. Gyrotron FU CW GIII gave a higher power, of up to 420 W. The higher power obtained from Gyrotron FU CW GIII was achieved using a new magnetron injection gun and by carefully setting the gyrotron position. Gyrotron FU CW GIII will be used as a power source for pulsed ESR experiments.

Acknowledgement This work was partly supported by a special fund for research projects from the Ministry of Education, Science, Sports and Culture of Japan.

References

1. Y. Tatematsu, Y. Yamaguchi, T. Idehara, T. Ozeki, R. Ikeda, T. Kanemaki, I. Ogawa, T. Saito, *J. Infrared Milli. Terahz. Waves* 33, 292 (2012).
2. T. Yamazaki, A. Miyazaki, T. Namba, S. Asai, T. Kobayashi, T. Suehara, Y. Tatematsu, I. Ogawa, T. Idehara, in “Extended abstracts of 38th IRMMW-THz” (2013) Fr1-5.
3. A. Miyazaki, T. Yamazaki, T. Suehara, T. Namba, S. Asai, T. Kobayashi, H. Saito, T. Idehara, I. Ogawa, Y. Tatematsu, *J. Infrared Milli. Terahz. Waves*, DOI 10.1007/s10762-013-0001-8 (2013).
4. T. Idehara and S.P. Sabchevski, *J. Infrared Milli. Terahz. Waves* 33, 667 (2012).
5. T. Yamazaki, A. Miyazaki, T. Suehara, T. Namba, S. Asai, T. Kobayashi, H. Saito, I. Ogawa, T. Idehara, S. Sabchevski, *Phys. Rev. Lett.* 108 253401 (2012).
6. L.R. Becerra, G. J. Gerfen, R. J. Temkin, D. J. Singel, R. Griffin, *Phys. Rev. Lett.* 71, 3561 (1993).
7. T. Idehara, I. Ogawa, L. Agusu, T. Kanemaki, S. Mitsudo, T. Saito, T. Fujiwara, H. Takahashi, *Int. J. Infrared Milli. Waves* 28, 433 (2007).
8. T. Idehara, K. Kosuge, La Agusu, I. Ogawa, H. Takahashi, M. E. Smith, R. Dupree, *J. Infrared Milli. Terahz. Waves* 31, 763 (2010).
9. T. Idehara, K. Kosuge, La Agusu, R. Ikeda, I. Ogawa, T. Saito, Y. Matsuki, K. Ueda, T. Fujiwara, *J. Infrared Milli. Terahz. Waves* 31, 775 (2010)
10. Y. Yamaguchi, Y. Tatematsu, T. Saito, R. Ikeda, J. C. Mudiganti, I. Ogawa, T. Idehara, *Plasma Fusion Res.* 7, 1205004 (2012).
11. Y. Yamaguchi, Y. Tatematsu, T. Saito, R. Ikeda, J. C. Mudiganti, I. Ogawa, T. Idehara, *Phys. Plasmas* 19, 113113 (2012).
12. Y. Tatematsu, Y. Yamaguchi, T. Idehara, T. Ozeki, T. Kawase, H. Kato, J. Aiba, R. Ikeda, T. Kanemaki, I. Ogawa, T. Saito, in “Proceedings of the 4th international workshop on far-infrared technologies 2012” (2012) 34.
13. O. Dumbrajs, *Int. J. Infrared Milli. Waves* 15, 1255 (1994).
14. N.A. Zavol’skiy, V. E. Zapevalov, M. A. Moiseev, A. S. Sedov, *Radiophys. Quantum Electron.* 54, 402 (2011).
15. Y. Tatematsu, T. Kawase, R. Ichioka, Y. Yamaguchi, I. Ogawa, R. Ikeda, T. Idehara, T. Saito, in “Extended abstracts of 38th IRMMW-THz” (2013) Tu1-5.